



Expression and regulation of RAD51 mediate cellular responses to chemotherapeutics

Zhengguan Yang^a, Alan S. Waldman^b, Michael D. Wyatt^{a,*}

^a Department of Pharmaceutical and Biomedical Sciences, South Carolina College of Pharmacy, University of South Carolina, Columbia SC 29208, United States

^b Department of Biological Sciences, University of South Carolina, Columbia SC 29208, United States

ARTICLE INFO

Article history:

Received 1 November 2011

Accepted 16 December 2011

Available online 24 December 2011

Keywords:

Thymidylate synthase
Homologous recombination
Replication protein A
RAD51
Etoposide

ABSTRACT

There is evidence that RAD51 expression associates with resistance to commonly used chemotherapeutics. Our previous work demonstrated that inhibitors of thymidylate synthase (TS) induced RAD51-dependent homologous recombination (HR), and depleting the RAD51 recombinase sensitized cells to TS inhibitors. In this study, the consequences of RAD51 over-expression were studied. Over-expression of wild-type RAD51 (~6-fold above endogenous RAD51) conferred resistance to TS inhibitors. In contrast, over-expression of a mutant RAD51 (T309A) that is incapable of being phosphorylated rendered cells more chemosensitive. Moreover, over-expression of the T309A mutant acted in a dominant negative manner over endogenous RAD51 by causing the reduced localization of RAD51 foci following treatment with TS inhibitors. To measure the effect of mutant RAD51 on the cellular response to other DNA damaging chemotherapeutics, the topoisomerase poison etoposide was utilized. Cells over-expressing wild-type RAD51 showed reduced DNA strand breaks, while cells over-expressing the mutant RAD51 showed more than twice as many strand breaks, suggesting that the mutant RAD51 was actively inhibiting strand break resolution. To directly demonstrate an effect on HR, wild-type RAD51 and T309A mutant RAD51 were transiently expressed in HeLa cells that contained an HR reporter construct. HR events provoked by DNA breaks induced by the I-SceI endonuclease increased in cells expressing wild-type RAD51 and decreased in cells expressing the T309A mutant. Collectively, the data suggest that interference with the activation of RAD51-mediated HR represents a potentially useful anticancer target for combination therapies.

© 2011 Elsevier Inc. All rights reserved.

1. Introduction

Homologous recombination (HR) is a critical means of repairing DNA double strand breaks, and defects in HR lead to chromosomal instability and cancer. More recently has it been realized that tumors with defects in specific components of HR (e.g., BRCA2) can be therapeutically targeted in a synthetic lethal manner [1,2]. The RAD51 recombinase is an essential component of eukaryotic HR. Changes in RAD51 expression affect the cellular response to chemotherapeutic agents that damage DNA, such as cisplatin, mitomycin C, and etoposide [3–6]. Inhibitors of thymidylate

synthase (TS) are widely used chemotherapeutic agents, and TS inhibition is known to cause S-phase arrest and DNA damage [7]. Transient depletion of RAD51 sensitized cells to raltitrexed (Tomudex[®]), an antifolate-based inhibitor of thymidylate synthase [8] or to capecitabine, the prodrug of 5-FU [9,10]. Raltitrexed also induced bona fide recombination events as measured by a model system in human fibroblasts, the first such direct demonstration that thymidylate deprivation causes recombination in mammalian cells [11].

Studies by us and others have shown that the ATR DNA damage signaling kinase and its key target, the CHK1 checkpoint kinase, are activated by TS inhibitors and influence chemosensitivity [8,12–15]. CHK1 has been shown to be required for HR, and to phosphorylate RAD51 at threonine 309 [16]. Replication protein A (RPA) is an important target of ATM and ATR, which phosphorylate the 32 kDa subunit (RPA2) of RPA at multiple sites in response to DNA damage and replication stress [17]. Phosphorylation of RPA2 by CHK1 was also shown to facilitate displacement of RPA from DNA, suggesting this was necessary to engage the strand invasion step of HR mediated by RAD51 [18,19]. We previously showed that TS inhibitors potently induced phosphorylation of RPA2,

Abbreviations: HR, homologous recombination; DSBs, DNA double strand breaks; TS, thymidylate synthase; RTX, raltitrexed (TomudexTM); 5-FU, 5-fluorouracil; FdUrd, fluorodeoxyuridine; UCN-01, 7-Hydroxy-staurosporine; GFP, green fluorescent protein.

* Corresponding author at: Department of Pharmaceutical and Biomedical Sciences, South Carolina College of Pharmacy, University of South Carolina, 715 Sumter Street, Columbia SC 29208, United States. Tel.: +1 803 777 0856; fax: +1 803 777 8356.

E-mail address: wyatt@sccp.sc.edu (M.D. Wyatt).

which strongly suggested that the DNA damage caused by TS inhibitors results in stalled and/or collapsed replication forks [8].

In this study, we further explore HR status and the response to chemotherapy by focusing on the key steps of RPA phosphorylation and recruitment of RAD51. HCT116 colorectal cancer cells were chosen as a model system for mismatch repair defective cancers, which are known from laboratory and clinical experience to be unresponsive to TS inhibitor treatments [20–22]. Cells with induced over-expression of either wild-type RAD51 or T309A mutant RAD51 were compared to cells with endogenous expression of RAD51. Collectively, our observations strongly suggest that RAD51-dependent HR influences the cellular response to TS inhibitors and might represent a point of attack in combination therapy with TS inhibitors.

2. Materials and methods

2.1. Reagents

Caffeine, 5-fluoro-deoxyuridine (FdUrd), 5-fluorouracil (5-FU), 7-hydroxystaurosporine (UCN-01), and other chemicals were from Sigma (St. Louis, MO). Raltitrexed (RTX, TomudexTM) was generously provided by AstraZeneca (U.K.). Anti-RPA32 (RPA2) monoclonal antibody was from Kamiya Biomedical (Seattle, WA). Anti-phospho-RPA2 (ser4/ser8) polyclonal antibody was from Bethyl Biotech Inc. (Montgomery, TX). Anti-Rad51 polyclonal antibody was from Santa Cruz Biotech (Santa Cruz, CA).

2.2. Cell culture and drug treatments

HCT116 colon cancer cells and HT-29 colon adenoma cancer cells were obtained from American Type Culture Collection (Manassas, VA). HCT116 cells were maintained at 37 °C and 5% CO₂ in McCoy's 5A medium (Hyclone, Logan UT) supplemented with 10% (v/v) fetal bovine serum (Hyclone) and 1% penicillin/streptomycin (Invitrogen, Carlsbad, CA). HT-29 cells were maintained at 37 °C and 5% CO₂ in Dulbecco's Modified Eagle's medium (Invitrogen) supplemented with 10% (v/v) fetal bovine serum (Hyclone) and 1% penicillin/streptomycin (Invitrogen). Exponentially growing cells (0.6×10^6) were seeded 24 h prior to each experiment. Medium was replaced with drug in fresh medium for dosages and times indicated, while medium lacking drug was used for mock treatments.

2.3. RAD51 expression constructs and transfection for stably expressing clones

The pLXSP and pLXSP-Rad51 plasmids were kindly provided by Shen and co-workers [23]. The mutant Rad51 T309A was generated by QuikChangeTM site-directed mutagenesis (formerly Strategene, now Agilent, Santa Clara, CA). The primers were (top) 5'-GGAAGAGGGGAAGCCAGAATCTGCAAATCTACG-3' and (bottom) 5'-CGTAGATTTTGCAGATTCTGGCTTCCCTCTTCC-3'. Plasmids were sequenced to confirm the appropriate substitution had been made. A total of 6×10^6 cells were transfected by electroporation with 2 µg of plasmid (400 V, 500 µF, >1000 Ω and 2 mm cuvette, Gene Pulser XcellTM, Bio-Rad, Hercules, CA). Following recovery for 48 h, transfected cells were selected by growth in media containing 100 µM puromycin for 14 days. Puromycin resistant clones that over-expressed Rad51 or mutant Rad51 were determined by Western blot, as described previously [8].

2.4. Cell viability, growth assays and cell cycle

Cell viability was determined by MTT assay and colony-forming assays as described [8,24–26]. IC₅₀ values were calculated by

plotting viability as a percent compared to untreated control. Cell cycle distribution was determined by flow cytometry as previously described [8,24,26]. DNA content was analyzed by using Cytomics FC-500 Flow Cytometer with CXP software version 2.2 (Beckman Coulter, Fullerton, CA) and quantitation of the cell cycle phases was performed using Modfit LT 3.2 (Verity Software House, Topsham, ME).

2.5. Immunofluorescence

Immunofluorescence was carried out as described in detail [8]. Primary antibodies were used at the following ratios: anti-RAD51, 1:500; anti-RPA2, 1:500. Secondary antibodies were Alexa Fluor 568 anti-mouse IgG and Alexa Fluor 488 anti-rabbit IgG utilized at a ratio of 1:250. Image data were captured with an Olympus X81 fluorescence microscope (Center Valley PA) and a 63X objective under oil. Olympus Metamorph[®] software was used to quantify data by counting foci number in at least 50 cells per sample, with a foci intensity of at least 30 intensity units. Cells were scored as positive for damage-induced foci if there were ≥ 5 spots per cell. The threshold levels to score foci as positive for co-localization were a foci size of at least four pixels and 200 intensity units. Co-localization was scored as a percent of the number of spots containing at least 25% yellow compared to the total number of RAD51 foci. The averaged data are from three independent experiments.

2.6. Comet assay

Alkaline comet assay was performed as previously described [25], with the following modifications. Cells were treated with etoposide (24 h) for the doses indicated then immediately harvested and processed. After electrophoresis, DNA was stained with SYBRTM Green (Invitrogen) and analyzed using HCSAv2 software (Loats, Gaithersburg MD).

2.7. HR events measured by I-SceI induction of GFP expression

The HeLa-DRGFP cells were a kind gift from Pierce et al. [27]. To introduce RAD51 expression constructs, 50 µg of purified pLXSP-Rad51 or pLXSP-M-Rad51 plasmid DNA (buffer only was used as the untreated control) was electroporated into 3×10^6 cells utilizing a Gene Pulser XcellTM and preset protocol for HeLa cells. After recovery for 48 h, 100 µg of pCBASce plasmid DNA was electroporated into 3×10^6 cells (buffer only was used for the untreated control). Following 48 h recovery, cells were processed for analysis by flow cytometry (FC-500 Flow Cytometer, Beckman, CA). To establish the parameters for the analysis protocol, parental HeLa cells were used as GFP negative, HeLa cells expressing a GFP-labeled Histone H2B were used as GFP positive [28], and HeLa-DRGFP cells electroporated with buffer alone were untreated controls. A minimum of 3×10^4 cells were counted in each sample and the percent of GFP positive cells quantified.

2.8. Data analysis

Quantification presented in bar graphs represents the mean \pm standard error of at least three independent experiments performed in duplicate. The Student's *t*-test was employed for pair-wise comparisons; a *p* value of <0.05 was considered to indicate statistical significance.

3. Results

To answer the question whether RAD51 overexpression renders cells chemoresistant, an expression construct for wild-type as well as an empty vector control were introduced. In addition, an

expression construct for a T309A mutant of RAD51 was generated to determine the importance of this CHK1 phosphorylation site [16]. It should be noted that attempts to isolate stable transfectants of the mutant RAD51 by selection in HeLa or HT-29 cells were unsuccessful, suggesting that mere expression of this mutant is lethal in these cell lines (data not shown). HCT116 colorectal cancer cells were utilized as a model of mismatch repair defective (microsatellite instability +) cancer that lacks the chromosomal instability of the other two cancer cell lines. Two independent HCT116 clones were evaluated for each transfection. The wild-type and mutant RAD51 proteins were over-expressed at similar levels in HCT116 cells in clone 1 for each (Fig. 1A), which was 6-fold higher than the endogenous RAD51 detected in cells containing the empty vector control. Note the exposure time of the blot that rendered the RAD51 bands in the over-expressed cells quantifiable makes the level of endogenous RAD51 in the vector only control cells appear faint by comparison. Clone 1 for each was used for subsequent experiments and all subsequent experiments were performed in cells within ten passages of the original selection. The HCT116 cells were treated with RTX and viability measured. The data show that the wild-type overexpressing cells were resistant to RTX, while the T309A overexpressing cells were sensitized to RTX, relative to the vector only controls with endogenous levels of RAD51 (Fig. 1B).

The formation of nuclear foci for RAD51 and RPA is thought to represent sites of active repair and were readily induced by RTX in HeLa and HT-29 cells [8]. In the present study, RAD51 foci were induced in HCT116 cells with empty vector (endogenous RAD51), cells expressing the wild-type, and cells expressing the mutant RAD51 (Representative images are shown in Supplementary Fig. 1). However, the percentage of cells with foci varied substantially among the sublines at same treatment of 30 nM RTX for 24 h. Specifically, 58% of the cells were positive for foci in the cells with empty vector, representing endogenous RAD51 foci (Fig. 2). Greater than 90% of the cells overexpressing wild-type RAD51

were positive, suggesting that the presence of additional exogenous RAD51 stimulates foci formation (Fig. 2). In contrast, the percentage of foci-positive cells dropped to 35% in the mutant-expressing cells, suggesting that mutant RAD51 inhibited foci induced by RTX in a dominant negative manner. RPA foci induced by RTX were evident in 75% of the cells over-expressing wild-type RAD51, while RPA foci were seen in 35% of the vector only control cells. Interestingly, the formation of RPA foci was greatly reduced in the mutant RAD51 over-expressing cells (Fig. 2), suggesting that the presence of mutant RAD51 suppresses the localization of RPA in response to TS inhibition. RAD51 and RPA did not completely co-localize following RTX treatment in this study or our previous work [8]. The extent of co-localization of the two proteins indicates sites in which the strand exchange step is occurring. The co-localization of RAD51 and RPA almost doubled when comparing the cells with empty vector (25%) versus wild-type RAD51 expressing (46%) cells, while almost no co-localization was observed in mutant RAD51 expressing cells due to the loss of RPA foci (Fig. 2).

Fig. 3A and B shows that phosphorylation of RPA2 (Ser4/Ser8) is caused by RTX and FdUrd, respectively, in parental HCT116 cells. Interestingly, low doses of caffeine increased RPA2 phosphorylation, a result reminiscent of that seen in HCT116 cells treated with hydroxyurea and caffeine [29]. At higher doses, RPA2 phosphorylation was reduced by co-treatment with caffeine. RPA2 phosphorylation and its inhibition by caffeine was also confirmed in HT-29 colorectal cancer cells (Fig. 3C and D), which had been examined in our previous study [8]. To confirm that caffeine did not affect the ability of TS inhibitors to block their target, we measured the covalent ternary complex of TS. Specifically, the active metabolite of fluoropyrimidines, FdUMP, is a suicide inhibitor of TS and is detected as a higher molecular weight species by PAGE and Western blotting. Note that RTX is a non-covalent, competitive inhibitor of the tetrahydrofolate cofactor, so its inhibition of TS cannot be detected in this manner. The complex of TS and FdUMP was readily detected following treatment with FdUrd or 5-FU and was unaffected by the addition of caffeine in either the HCT116 or HT-29 cells (Fig. 4A and B, respectively), showing that caffeine was not directly affecting TS inhibition.

UCN-01 was utilized as an inhibitor of CHK1 to determine the role of this crucial effector kinase as it relates to RPA and RAD51 [19,30]. UCN-01 suppressed the RPA phosphorylation in HT-29 cells that was induced by RTX (Supplementary Fig. 2A) or FdUrd (Supplementary Fig. 2B). In previous experiments, we have shown RTX potently induces S-phase arrest, approaching 100% of the population [8,24,26]. UCN-01 also induces an S-phase arrest [30], so cell cycle studies were performed to determine the effect of combining the agents. Treatment with RTX alone induced an S-phase population of 98.1%, and co-incubation with UCN-01 did not

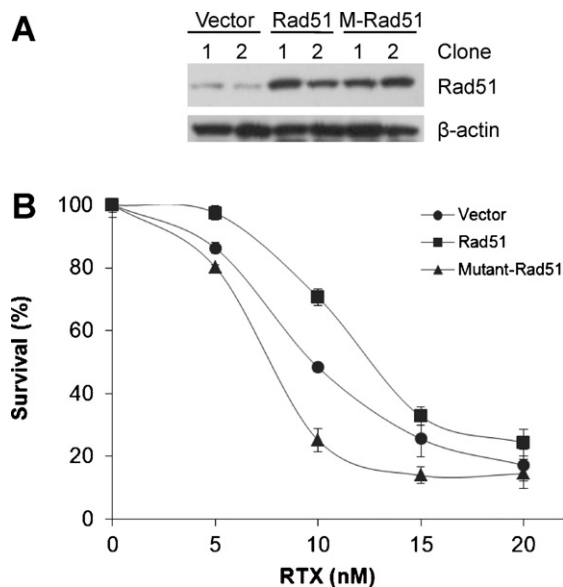


Fig. 1. RAD51 overexpression and sensitivity to TS inhibition. (A) Western blot showing RAD51 in two clones each of HCT116 cells transfected with an empty vector (lanes 1 and 2), wild-type RAD51 (lanes 3 and 4) and T309A RAD51 mutant. (B) HCT116 cells with empty vector (●), wild-type RAD51 (■), and mutant RAD51 (▲) were treated with increasing concentrations of RTX for 24 h and viability was measured by MTT assay after 3 additional day's incubation in drug free medium. Data are plotted as percent survival compared to untreated control and are the mean (\pm s.d.) of four independent experiments.

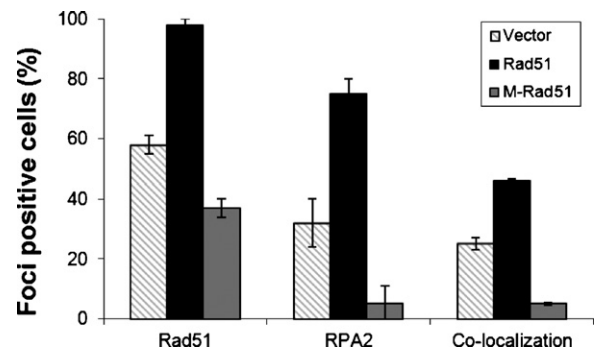


Fig. 2. RAD51 and RPA2 foci formation induced by treatment with 30 nM RTX for 24 h. HCT116 cells with empty vector (grey stripe bars), wild-type RAD51 (black bars), and mutant RAD51 (grey bars) were treated with RTX for 24 h prior to fixation and immunostaining. The Y-axis represents the percentage of cells scored positive for foci (Section 2) relative to the total number of cells viewed.

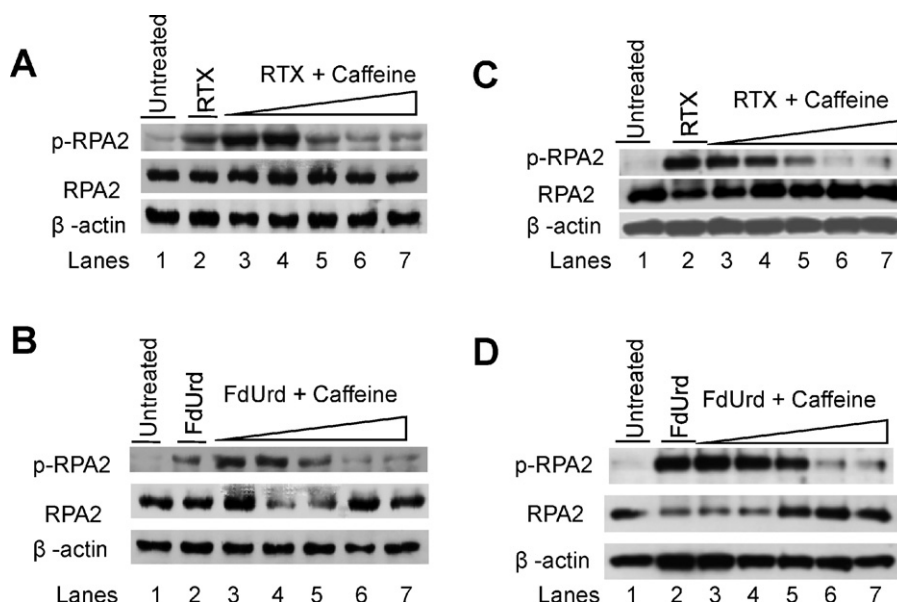


Fig. 3. Western blots showing that RPA2 phosphorylation (Ser4/Ser8) induced by TS inhibitors is blocked by caffeine in HCT116 (A, B) and HT-29 (C, D) cells. Cells were treated with RTX (30 nM, A, C) or FdUrd (1 μ M, B, D) for 24 h. TS inhibitors were co-incubated with caffeine at a concentration of 0.25, 0.5, 1, 2, and 4 mM in lanes 3, 4, 5, 6 and 7, respectively. A representative blot of three independent repeats is shown.

alter this S-phase arrest (Supplementary Fig. 3, left panels). It should be noted that a peak of cells with $>4n$ DNA content became noticeable, which we speculate might represent endoreduplication events in a small proportion of the cells and were not included in the Modfit analysis of cell cycle distribution. Following 24 h recovery, 9.7% of the cells treated with RTX alone progressed to G2/M, while 100% of cells treated with RTX and UCN-01 remained in S-phase (Supplementary Fig. 3). It should also be noted that the proportion of events calculated by ModFit as “debris” increased from 6.4% with RTX alone to 13.0% with RTX plus UCN-01, which suggested an enhanced chemosensitization was occurring. It was previously reported that combining 5-FU or fluorodeoxyuridine with UCN-01 increased efficacy of the drugs [31,32]. We observed that co-incubating UCN-01 with RTX increased the chemosensitivity of HT-29 cells by almost double (Supplementary Fig. 4, compare RTX alone to RTX + UCN-01), confirming that UCN-01 in

combination with nucleotide- or folate-based inhibitors of TS is more potent than the individual agents alone.

To determine whether wild-type RAD51 and mutant RAD51 overexpression influenced the cellular response to another chemotherapeutic agent, the topoisomerase II poison etoposide was utilized. The alkaline comet assay was utilized to measure single and double strand breaks in the cells over-expressing wild-type or mutant RAD51 compared to cells containing the empty vector and endogenous RAD51. In Fig. 5, etoposide-induced strand breaks as measured by tail moment increased in a dose-dependent manner in all three sublines from 2.5-fold up to 4.5 fold following treatment. However, the extent of DNA damage was greatest in cells expressing the mutant RAD51, while cells expressing wild-type RAD51 showed a greater than 2-fold reduction in damage following etoposide treatment compared to the comet tail moments seen in mutant RAD51 expressing cells at the same

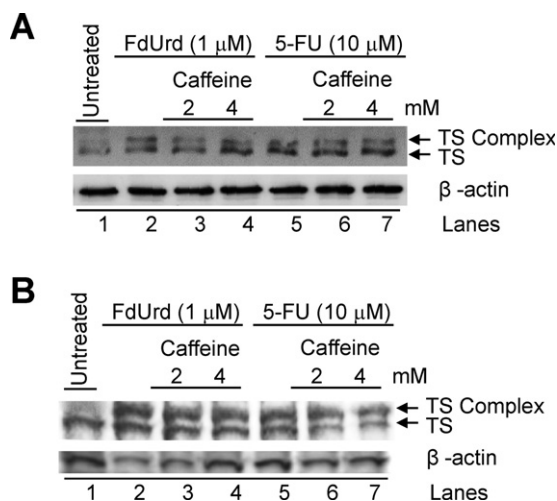


Fig. 4. Western blots showing that the presence of caffeine does not alter inhibition of TS. The covalent ternary complex of TS is detected as the upper band in extracts from HCT116 (A) and HT-29 (B) cells treated with FdUrd or 5-FU for 24 h. The presence of caffeine does not alter the extent of ternary complex formation and TS inhibition.

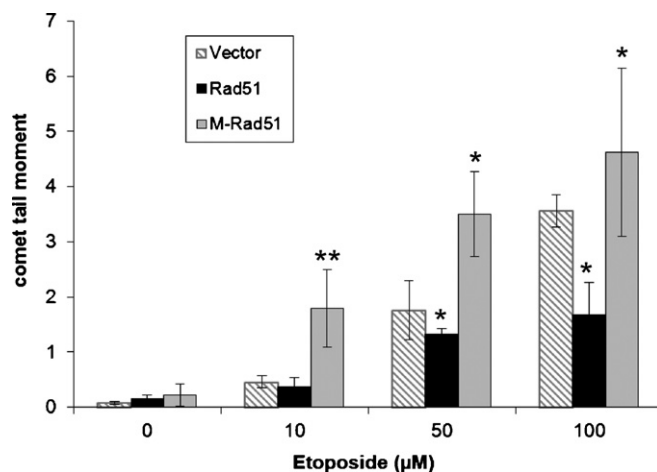


Fig. 5. DNA damage as measured by the comet assay. HCT116 cells with empty vector (grey stripe bars), wild-type RAD51 (black bars), and mutant RAD51 (grey bars) were treated with the indicated doses of etoposide for 24 h. Pairwise comparison by *t*-test was between vector only samples and wild-type RAD51 or mutant RAD51 samples at the same doses of etoposide. ** represents $P < 0.01$ and * represents $P < 0.05$.

etoposide doses. In other words, the data suggest that over-expression of wild-type RAD51 in these cells promote resolution of etoposide-induced strand breaks, while over-expression of the mutant RAD51 actively inhibits strand break resolution in a dominant negative manner.

To directly demonstrate that the mutant T309A RAD51 acts in a dominant negative manner to suppress HR, experiments were performed in cells containing a chromosomally integrated DRGFP recombination reporter (HeLa DRGFP) as described in detail [27]. Expression of I-SceI endonuclease introduces a DSB in the SceGFP gene, and repair by HR reconstitutes a functional GFP gene and GFP expression. HeLa DRGFP cells were electroporated with the expression constructs for wild-type RAD51 or mutant RAD51 (buffer only for the control cells) and allowed to recover for 48 h to allow for RAD51 expression. Cells were counted, and lysates prepared from a portion of the cells were analyzed for RAD51 expression (Fig. 6A). Wild-type and mutant RAD51 expression was elevated approximately 1.5 fold compared to endogenous RAD51 in the HeLa cells (Fig. 6A), which confirms over-expression under these transient transfection conditions. Interestingly, a profound drop in cell number was clearly evident when the mutant RAD51 was transfected into HeLa cells. There was an average of a 6-fold loss in cell numbers recovered from electroporation with the mutant RAD51 vector ($n = 6$ experiments), and there was a 2-fold loss in cell numbers following electroporation with wild-type RAD51 vector in comparison to the numbers of cells electroporated with buffer only. Following 48 h recovery, cells were electroporated with the pCBASce plasmid (or buffer only for the negative control) to express the I-SceI endonuclease and induce DSBs. After

a second 48 h recovery, GFP positive cells were measured by flow cytometry (Section 2). Fig. 6B shows the average of two experiments in which the cell numbers recovered was high enough for flow cytometry analysis. Supplementary Fig. 5 shows the dot plots from one experiment. The percentage of GFP positive cells was 1.1% for those electroporated with buffer alone. Electroporation of the I-SceI endonuclease induced a GFP-positive population of 14.0%. Cells in which wild-type RAD51 was expressed prior to I-SceI displayed a GFP-positive population of 16.5%, demonstrating that there was a measurable increase in HR events in the cells over-expressing RAD51. In contrast, cells in which mutant RAD51 was expressed prior to I-SceI displayed a GFP-positive population of 12.7%. In summary, the mutant RAD51 appeared to suppress error free HR in this assay, whereas the over-expression of wild-type promoted HR.

4. Discussion

The role of HR in cancer initiation and treatment is currently best exemplified with BRCA2 defective breast cancer and treatment with PARP inhibitors [33,34]. The role of HR dysfunction in sporadic cancer is also being pursued. For example, PARP inhibitors are now being tried in patients with metastatic “triple negative” breast cancers, which have a poorer prognosis than ER+ or HER2+ cancers [35]. Much more remains to be explored regarding the possibility of targeting other participants in DNA damage responses and HR. Our previous work established that RAD51-dependent HR is invoked by treatment with TS inhibitors [8,11]. In this study, we provide evidence that elevated expression of RAD51 increased resistance to TS inhibitors, which are used in the treatment of over a third of all cancer cases, including breast, lung, and colorectal cancer. Although mammalian RAD51 is essential for proliferation, it is becoming apparent that its aberrant expression is problematic [4], and consequently there are recent efforts to develop inhibitors of RAD51. For example, high throughput screening has identified inhibitors of RAD51 [36], and a natural product sensitized cells to capecitabine by down-regulating RAD51 expression, among other gene products [10].

The data here also showed that interfering with the regulation of key steps in HR, namely phosphorylation of RAD51 and RPA, caused chemosensitization. Overexpression of the T309A mutant of RAD51, which is incapable of being phosphorylated by CHK1, sensitized cells to RTX in a dominant negative manner in the HCT 116 cells. Attempts to isolate stable transfectants of the mutant RAD51 by selection in HeLa or HT-29 cells were unsuccessful (data not shown), suggesting that cancer cell lines with chromosomal instability cannot tolerate the expression of this mutant. The reduction in RAD51 and RPA-associated foci caused by the presence of mutant RAD51 suggests it directly interfered with the initiation and/or progression of HR, which is in agreement with observations of others following hydroxyurea treatment [16]. The results also showed that RPA2 phosphorylation induced by TS inhibitors was inhibited by caffeine or UCN-01, which suggests that ATM/ATR/DNA-PK and/or the downstream target CHK1 are phosphorylating RPA2 in response to TS inhibition. RPA can also be phosphorylated by CHK1 [19], and the data here showed that UCN-01 prevented the phosphorylation of RPA2 induced by TS inhibitors. UCN-01 treatment induces replicational stress presumably by blocking the initiation of HR invoked by spontaneous collapsed replication forks [30]. UCN-01 prevented a resumption of S-phase progression upon removal of RTX during recovery (Supplemental Fig. 3), which suggests that the enhanced chemosensitivity seen with UCN-01 and TS inhibitors in combination may be via simultaneous induction of damage that invokes HR and the inhibition of HR activation by CHK1.

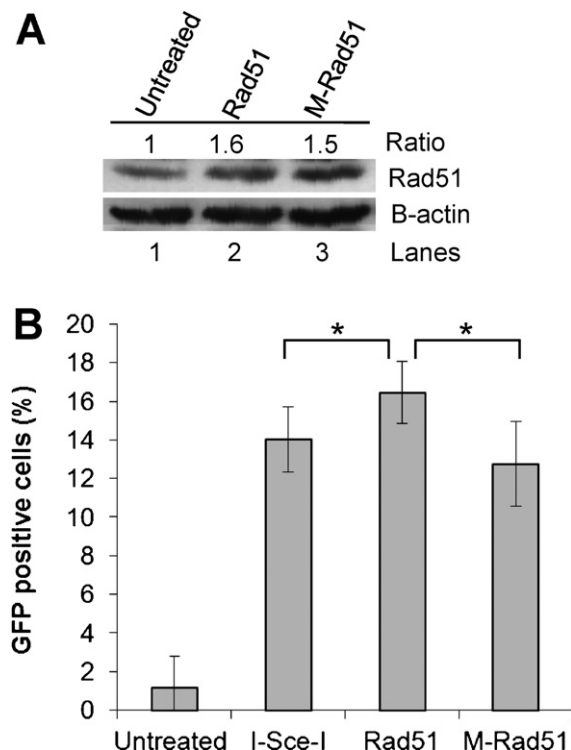


Fig. 6. Measurement of HR by reconstitution of GFP fluorescence in HeLa DRGFP cells. (A) Western blot of RAD51 levels in cells 48 h after electroporation with buffer alone (untreated), or the expression construct for wild-type or mutant RAD51. (B) Bar graph showing the percentage of GFP positive cells (average of two experiments) after electroporation with buffer followed 48 h later by buffer (untreated), buffer followed 48 h later by the I-SceI expression construct (I-SceI), wild-type RAD51 followed 48 h later by I-SceI, or mutant RAD51 followed 48 h later by I-SceI. See Section 2 for a detailed description of the experimental procedure. Pairwise comparison by *t*-test was between wild-type RAD51 and vector only or mutant RAD51 samples. * Represents $P < 0.05$.

The topoisomerase II poison etoposide was examined because it was previously shown that RAD51 levels correlate with sensitivity to etoposide [3] and knockdown of RAD51 sensitized cells to this agent [5]. Strand breaks as measured by the comet assay were reduced in the wild-type RAD51 over-expressing cells, while strand breaks increased in comparison by 2-fold in the mutant-RAD51 over-expressing cells. In other words, the presence of the mutant RAD51 seemed to directly interfere with the resolution of DNA damage and/or repair intermediates, while overexpression of the wild-type protein promoted resolution. The results with the DRGFP cells directly demonstrate that wild-type RAD51 expression increased error free HR provoked by I-SceI induced DSBs, whereas mutant T309A RAD51 expression decreased HR and likely acts in a dominant negative fashion. To our knowledge, this is the first demonstration that interfering with the regulation of RAD51 by phosphorylation at this site interferes with the resolution of strand breaks by HR. The results with etoposide and TS inhibitors suggest that RAD51 status can alter the efficacy of treatment to multiple types of chemotherapy, and that targeting HR could enhance their efficacy.

The promise of all new, molecularly targeted chemotherapeutic agents that enter the market is tempered by acquired resistance mechanisms. For example, BRCA2 defective tumor cells can acquire resistance to PARP inhibitors via an intragenic deletion of the frameshift mutation that restores an open reading frame of BRCA2 and HR activity [37]. New agents will inevitably be utilized in combination with traditional cytotoxic drugs to reduce the likelihood of resistance occurring. Our studies suggest that there would be benefit in combining TS inhibitors with novel kinase inhibitors that target the DNA damage response.

Acknowledgements

This research was supported in part by a grant from the NIH/NCRF to the Center for Colon Cancer Research (P20 RR17698) and from the NIH/NCI to MDW (R01 CA100450). Drs. Doug Pittman and Sondra Berger are acknowledged for helpful discussions.

Appendix A. Supplementary data

Supplementary data associated with this article can be found, in the online version, at doi:10.1016/j.bcp.2011.12.022.

References

- [1] Bryant HE, Schultz N, Thomas HD, Parker KM, Flower D, Lopez E, et al. Specific killing of BRCA2-deficient tumours with inhibitors of poly(ADP-ribose) polymerase. *Nature* 2005;434:913–7.
- [2] Farmer H, McCabe N, Lord CJ, Tutt AN, Johnson DA, Richardson TB, et al. Targeting the DNA repair defect in BRCA mutant cells as a therapeutic strategy. *Nature* 2005;434:917–21.
- [3] Hansen LT, Lundin C, Spang-Thomsen M, Petersen LN, Helleday T. The role of RAD51 in etoposide (VP16) resistance in small cell lung cancer. *Int J Cancer* 2003;105:472–9.
- [4] Klein HL. The consequences of Rad51 overexpression for normal and tumor cells. *DNA Repair (Amst)* 2008;7:686–93.
- [5] Schonn I, Hennesen J, Dartsch DC, Ku70 and Rad51 vary in their importance for the repair of doxorubicin- versus etoposide-induced DNA damage. *Apoptosis* 2011;16:359–69.
- [6] Slupianek A, Schmutte C, Tomblin G, Nieborowska-Skorska M, Hoser G, Nowicki MO, et al. BCR/ABL regulates mammalian RecA homologs, resulting in drug resistance. *Mol Cell* 2001;8:795–806.
- [7] Berger SH, Pittman DL, Wyatt MD. Uracil in DNA: consequences for carcinogenesis and chemotherapy. *Biochem Pharmacol* 2008;67:697–706.
- [8] Yang Z, Waldman AS, Wyatt MD. DNA damage and homologous recombination signaling induced by thymidylate deprivation. *Biochem Pharmacol* 2008;76:987–96.
- [9] Ko JC, Su YJ, Lin ST, Jhan JY, Ciou SC, Cheng CM, et al. Suppression of ERCC1 and Rad51 expression through ERK1/2 inactivation is essential in emodin-mediated cytotoxicity in human non-small cell lung cancer cells. *Biochem Pharmacol* 2011;79:655–64.
- [10] Ko JC, Tsai MS, Kuo YH, Chiu YF, Weng SH, Su YC, et al. Modulation of Rad51, ERCC1, and thymidine phosphorylase by emodin result in synergistic cytotoxic effect in combination with capecitabine. *Biochem Pharmacol* 2011;81:680–90.
- [11] Waldman BC, Wang Y, Kilaru K, Yang Z, Bhasin A, Wyatt MD, et al. Induction of intrachromosomal homologous recombination in human cells by raltitrexed, an inhibitor of thymidylate synthase. *DNA Repair* 2008;7:1624–35.
- [12] Parsels LA, Parsels JD, Tai DC, Coughlin DJ, Maybaum J. 5-fluoro-2'-deoxyuridine-induced cdc25A accumulation correlates with premature mitotic entry and clonogenic death in human colon cancer cells. *Cancer Res* 2004;64:6588–94.
- [13] Robinson HM, Jones R, Walker M, Zachos G, Brown R, Cassidy J, et al. Chk1-dependent slowing of S-phase progression protects DT40 B-lymphoma cells against killing by the nucleoside analogue 5-fluorouracil. *Oncogene* 2006;25:5359–69.
- [14] Wilsker D, Bunz F. Loss of ataxia telangiectasia mutated- and Rad3-related function potentiates the effects of chemotherapeutic drugs on cancer cell survival. *Mol Cancer Ther* 2007;6:1406–13.
- [15] Xiao Z, Xue J, Sowin TJ, Zhang H. Differential roles of checkpoint kinase 1, checkpoint kinase 2, and mitogen-activated protein kinase-activated protein kinase 2 in mediating DNA damage-induced cell cycle arrest: implications for cancer therapy. *Mol Cancer Ther* 2006;5:1935–43.
- [16] Sorensen CS, Hansen LT, Dziegielewska J, Syljuasen RG, Lundin C, Bartek J, et al. The cell-cycle checkpoint kinase Chk1 is required for mammalian homologous recombination repair. *Nat Cell Biol* 2005;7:195–201.
- [17] Binz SK, Sheehan AM, Wold MS. Replication protein A phosphorylation and the cellular response to DNA damage. *DNA Repair (Amst)* 2004;3:1015–24.
- [18] Liu JS, Kuo SR, Melendy T. Phosphorylation of replication protein A by S-phase checkpoint kinases. *DNA Repair (Amst)* 2006;5:369–80.
- [19] Sleeth KM, Sorensen CS, Issaeva N, Dziegielewska J, Bartek J, Helleday T. RPA mediates recombination repair during replication stress and is displaced from DNA by checkpoint signalling in human cells. *J Mol Biol* 2007;373:38–47.
- [20] Carethers JM, Chauhan DP, Fink D, Nebel S, Bresalier RS, Howell SB, et al. Mismatch repair proficiency and in vitro response to 5-fluorouracil. *Gastroenterology* 1999;117:123–31.
- [21] Meyers M, Wagner MW, Mazurek A, Schmutte C, Fishel R, Boothman DA. DNA mismatch repair-dependent response to fluoropyrimidine-generated damage. *J Biol Chem* 2005;280:5516–26.
- [22] Sargent DJ, Marsoni S, Monges G, Thibodeau SN, Labianca R, Hamilton SR, et al. Defective mismatch repair as a predictive marker for lack of efficacy of fluorouracil-based adjuvant therapy in colon cancer. *J Clin Oncol* 2010;28:3219–26.
- [23] Wray J, Liu J, Nickoloff JA, Shen Z. Distinct RAD51 associations with RAD52 and BCCIP in response to DNA damage and replication stress. *Cancer Res* 2008;68:2699–707.
- [24] Li L, Berger SH, Wyatt MD. Involvement of base excision repair in response to therapy targeted at thymidylate synthase. *Mol Cancer Ther* 2004;3:747–53.
- [25] Li L, Connor EE, Berger SH, Wyatt MD. Determination of apoptosis, uracil incorporation, DNA strand breaks, and sister chromatid exchanges under conditions of thymidylate deprivation in a model of BER deficiency. *Biochem Pharmacol* 2005;70:1458–68.
- [26] Luo Y, Walla M, Wyatt MD. Uracil incorporation into genomic DNA does not predict toxicity caused by chemotherapeutic inhibition of thymidylate synthase. *DNA Repair (Amst)* 2008;7:162–9.
- [27] Pierce AJ, Johnson RD, Thompson LH, Jasin M. XRCC3 promotes homology-directed repair of DNA damage in mammalian cells. *Genes Dev* 1999;13:2633–8.
- [28] Kanda T, Sullivan KF, Wahl GM. Histone-GFP fusion protein enables sensitive analysis of chromosome dynamics in living mammalian cells. *Curr Biol* 1998;8:377–85.
- [29] Cortez D. Caffeine inhibits checkpoint responses without inhibiting the ataxia-telangiectasia-mutated (ATM) and ATM- and Rad3-related (ATR) protein kinases. *J Biol Chem* 2003;278:37139–45.
- [30] Syljuasen RG, Sorensen CS, Hansen LT, Fugger K, Lundin C, Johansson F, et al. Inhibition of human Chk1 causes increased initiation of DNA replication, phosphorylation of ATR targets, and DNA breakage. *Mol Cell Biol* 2005;25:3553–62.
- [31] Grem JL, Danenberg KD, Kao V, Danenberg PV, Nguyen D. Biochemical and molecular effects of UCN-01 in combination with 5-fluorodeoxyuridine in A431 human epidermoid cancer cells. *Anticancer Drugs* 2002;13:259–70.
- [32] Hsueh CT, Kelsen D, Schwartz GK. UCN-01 suppresses thymidylate synthase gene expression and enhances 5-fluorouracil-induced apoptosis in a sequence-dependent manner. *Clin Cancer Res* 1998;4:2201–6.
- [33] Fong PC, Yap TA, Boss DS, Carden CP, Mergui-Roelvink M, Gourley C, et al. Poly(ADP)-ribose polymerase inhibition: frequent durable responses in BRCA carrier ovarian cancer correlating with platinum-free interval. *J Clin Oncol* 2010;28:2512–9.
- [34] Lord CJ, Ashworth A. Targeted therapy for cancer using PARP inhibitors. *Curr Opin Pharmacol* 2008;8:363–9.
- [35] O'Shaughnessy J, Osborne C, Pippen JE, Yoffe M, Patt D, Rocha C, et al. Iniparib plus chemotherapy in metastatic triple-negative breast cancer. *N Engl J Med* 2011;364:205–14.
- [36] Huang F, Motlekar NA, Burgwin CM, Napper AD, Diamond SL, Mazin AV. Identification of specific inhibitors of human RAD51 recombinase using high-throughput screening. *ACS Chem Biol* 2011;6:628–35.
- [37] Edwards SL, Brough R, Lord CJ, Natrajan R, Vatcheva R, Levine DA, et al. Resistance to therapy caused by intragenic deletion in BRCA2. *Nature* 2008;451:1111–5.